

# Study on pure oxygen exhaust gas combustion: key technology of CO<sub>2</sub> capture for high temperature fuel cell with coal syngas

Hanlin Wang (✉ [hanlin.wang.a@chnenergy.com.cn](mailto:hanlin.wang.a@chnenergy.com.cn))

National Institute of Clean and Low-Carbon Energy

**Qilong Lei**

Shenhua New Energy Company. Ltd.

**Pingping Li**

National Institute of Clean and Low Carbon Energy

**Changlei Liu**

Shenhua New Energy Company. Ltd.

**Yunpeng Xue**

National Institute of Clean and Low Carbon Energy

**Xuwei Zhang**

Shenhua New Energy Company. Ltd.

**Chufu Li**

National Institute of Clean and Low Carbon Energy

**Zhibin Yang**

China University of Mining and Technology

---

## Research

**Keywords:** IGFC system, Solid oxide fuel cell, Anode exhaust gas treatment, CO<sub>2</sub> capture, Oxy-combustion

**Posted Date:** January 12th, 2021

**DOI:** <https://doi.org/10.21203/rs.3.rs-33796/v3>

**License:**   This work is licensed under a Creative Commons Attribution 4.0 International License.

[Read Full License](#)

---

# Abstract

IGFC based on high temperature SOFC coupled with CO<sub>2</sub> capture process provides a new technology route of high efficiency and nearly zero CO<sub>2</sub> emission power system. Flame burning is an ideal method for tail gas treatment. In this paper, an oxy-combustor for a gross 10kW IGFC system anode exhaust gas is experimentally and numerically studied. Simulation method is verified by experiments. Key performances of the combustor are studied under different system process design conditions. 315K might be an ideal condensation temperature before burning for flame stability. CO could be almost fully converted under flame burning condition. CO<sub>2</sub> concentration after burning is over 0.958 when excess O<sub>2</sub> is less than 5%. Overall, 5% excess O<sub>2</sub> could be recommended for CO<sub>2</sub> gathering and environmental consideration. An optimal tangential angle exists around 25° for liner temperature controlling. Total fuel utilization percent had better be high enough to make oxygen flame temperature of anode exhaust gas lower than 1800K to make systems environment friendly. The results would be of great value to IGFC and CO<sub>2</sub> capture combined system designing.

## 1. Introduction

With consumption of non-renewable resource increasing, higher efficiency of power system is required. Fossil fuel combustion causes greenhouse effects. Integrated gasification fuel cell (IGFC) (Al-Khori et al. 2020) provides a new technology route to a power system. Compared with traditional coal utilization power generation systems, it has higher efficiency in theory. For IGFC, solid oxide fuel cell (SOFC) could be suitable as it has wider fuel flexibility and could be directly fed by syngas (Wu et al. 2020). Moreover, coupled with potential simple capturing process, a nearly zero greenhouse gas (CO<sub>2</sub>) releasing system with lower energy penalties and cost of capture relative to conventional system could be gained through IGFC system based on SOFC (Thallam Thattai et al. 2017). Carbon element in anode off-gas should be gathered to gain a high CO<sub>2</sub> capture rate. SOFC with high fuel utilization percent (Pirasaci, 2019) accomplishes CO<sub>2</sub> gathering inside stack. For some small systems with high fuel efficiency fuel cells, such as BlueGen system of SOLIDpower Company, fuel mass flow could pass the stacks through a single way (Ferreira et al. 2019), which make system simple. In addition, CO<sub>2</sub> could be gathered by specific complex system design. In some systems, anode off-gas looping through ejectors is taken into consideration to increase fuel utilization, which would certainly increase exhaust CO<sub>2</sub> density (Wang et al. 2020). For SOFC system, a certain amount of steam is needed blended into fuel before entering stacks to avoid carbon formation or to participate in the reforming reaction for system fueled with CH<sub>4</sub>. In system with anode looping, steam is provided by anode off-gas. But for anode single pass system like Bluegen, some extra is imported steam directly. Different system designs, fuel components and fuel utilization ratios may lead to difference in exhaust gas components. The off-gas treatment system should have good performance for relatively wide variation range of species mole fraction to improve the system adaption.

There may still exist about 10%-15% combustible component mainly consisting of CO and H<sub>2</sub> in exhaust gas with calorific value about 2-3 MJ/Nm<sup>3</sup>. Thus, further measures are needed not only for CO<sub>2</sub> capturing efficiency but also for waste heat utilization and environment requirements. Generally, exhaust gas needs to be completely oxidized to CO<sub>2</sub> and H<sub>2</sub>O. Spallina et al. (2018) proposed chemical looping combustion to deal with exhaust gas. Anode off-gas was imported to a fuel reactor and looping in it through ejectors. Off-gas reacted with the cathode inlet air through oxidizer carrier. The inlet air was heated up to 730°C before entering cathode by the exothermic oxidation reaction. Application of ejectors increased the difficulty of flow controlling. Chemical looping system could be expensive. Furthermore, it may not still achieve the desired rate of CO<sub>2</sub> gathering.

Oxy-combustion has been proved to be an effective method for CO<sub>2</sub> concentrating in some traditional power system (Francisco et al. 2016). Compared with air combustion, no extra impurity like N<sub>2</sub> is imported to the production, which may decrease the capture rate and increase compression energy required to pressurize the captured CO<sub>2</sub> for storage. As for IGFC, pure O<sub>2</sub> could be easily obtained from air separators used for the coal gasification process, which made oxy-combustion convenient to accomplish. To realize the exhaust gas oxy-combustion, a detailed combustor structure and exhaust gas dealing process design are needed.

Catalytic oxy-combustion is often used to deal with CO pollutant in power system exhaust gas. Chen et al. (2019) showed that TiO<sub>2</sub>-CuO was an effective catalyst for exhaust gas with 1.5% CO. If specific surface area was sufficient, the conversion could be over 90% in 7 hours. Han et al. (2016) showed that nickel oxide catalysts could combust the exhaust gas with a CO content level under 1% by volume at different temperature. The characteristic temperature was up to 600°C at lab-scale space velocity and no deactivation of catalysts for CO oxidation for just 720 min. Dey et al. (2020) proposed a detailed catalytic combustor for CO when testing Pt catalytic activity, which had a representative porous catalyst bed to increase specific surface. Most catalyst is applied to deal with exhaust gas which contains CO less than 1% by vol. It means that catalyst might just be suitable to deal with the off-gas CO within pollutant content level. However, SOFC exhaust gas contains far more CO and H<sub>2</sub>. And the gas flow rate could be larger than lab-scaled. This may lead to high local combustion temperature which is harmful to catalyst activity. Sufficient specific surface area is required for catalytic combustion which makes burner scale-up difficult. Pressure of anode gas should be strictly limited because it is to the disadvantage of fuel cell sealing. Pressure of off-gas may not be sufficient for the porous catalyst bed. These might make it unsuitable to apply catalytic oxy-combustion into practical system.

Direct pure oxygen flame burning shows another way to deal with the anode exhaust gas, which could almost fully convert CO to CO<sub>2</sub>. The main characters of exhaust gas are extremely high level moisture content and low calorific value. These characters may respectively challenge the flame stability and ignition. Ning et al. (2018) reported that water vapor and carbon dioxide increased the ignition temperature of H<sub>2</sub>/O<sub>2</sub> flame, which both steam and carbon dioxide show some negative effects on it. It means that a cooling dewatering process of anode off-gas should be carried out before flame

combustion. Recent researches proved that pure oxygen flame could be steady under extremely low equivalence ratio especially for  $H_2$  enriched fuel, which means it might have good performance for low-calorific exhaust gas. Rashwan et al. (2017) showed that oxygen partially premixed flame of natural gas could be steady in equivalence ratio range from 0.7-1.1. Imteyaz et al. (2018) showed similar results on  $H_2$  enriched methane oxygen premixed combustion. Besides, it was shown that  $H_2$  could decrease the lower limited equivalence ratio down to 0.2. Li et al. (2018) gained a stable oxy-methane premixed flame with  $O_2$  mole fraction from 0.25 to 1.0. And stability increased when  $O_2$  mole fraction increased. Too much excessive  $O_2$  would decrease  $CO_2$  concentration in production although it improves flame stability. Ilbas et al. (2019) studied oxy-combustion of low-calorific syngas numerically and experimentally. It is indicated that oxygen flame could almost burn out all the CO content even in low-calorific syngas even in low calorific gas. But flame burning may cause problems on  $NO_x$  emissions. Pollutant emission was related to flame temperature and burner design. Pollutant should be taken into consideration during system design because acidic gas may be harmful to systems and environment.

According to the above, for integrated system design, condensation process of anode off-gas would surely lead to heat loss. This makes it meaningful to discuss a proper condensation temperature for exhaust gas oxy-combustion to avoid undercooling. A reliable burner, which could reach a satisfactory CO converting rate, is needed. Amount of excessive  $O_2$  is worth to study to balance the flame stability, converting rate and  $CO_2$  concentration. Exhaust gas should be burnt around equivalence ratio which leads to high local flame temperature. In long-life systems, it is important control thermal creep deformation of combustor liner which is influenced by the inner jet flow and cooling strength. Differing from air combustor, oxidizer gas could not be directly used as liner cooling medium through method such as film cooling (Topal et al. 2019) since quantity of  $O_2$  for exhaust gas burning is rather small. Therefore, liner forced cooling should be involved. It decreases flame temperature and then CO converting rate. And drivers of forced cooling will increase inner consumption of the energy system. Moreover, high reacting temperature of oxy-combustion leads to high level  $NO_x$  emission possibility since  $N_2$  still exists both in industry syngas (Schluckner et al. 2020) and oxygen (Khallaghi et al. 2020).

Most commercial flat plate SOFC systems consist of some fuel cell generation modules. The module could be integrated by few large stacks, such as FuelCell Company with a single stack of 12.5kW, or numerous small stacks, such as BloomEnergy Company with a single stack of 1kW. Systems with 10kW power capacity could be considered as a modularization subsystem both for a single large stack and for several small stacks during system design. It could be convenient to enlarge the system to 100kW or MW level. Therefore, in this paper, a lab-scaled anode off-gas concept oxy-combustor for an IGFC system of 10kW gross power capacity is experimentally and numerically studied. Computational fluid dynamics (CFD) and chemical reactor network (CRN) method are verified and used to simulate the flame and emissions of combustor. Flame ignition of exhaust gas and pure oxygen under different condensation temperature is discussed. Then effects of excessive  $O_2$  and liner cooling on CO conversion rate are investigated. Influences of jet flow and outside forced cooling operating conditions on liner temperature are also analyzed. Pollutant emissions of different anode processing under different excess  $O_2$  amount

are also studied. The results could be very helpful for the integrated IGFC coupled with CO<sub>2</sub> capturing system design.

## 2. Experimental Setup

Fig. 1 shows the lab-scaled exhaust gas concept oxy-combustor which mainly consists of a flame chamber, a flame stabilizer, oxygen swirler and fuel swirling jet. All components are made of high temperature steel. The tangential angle of fuel jet is 25°. Swirlers and stabilizer provide a flow field with swirl and back flow which could improve mixing process and be beneficial to stability of flame root. Cooling air enter cooling chamber to cool flame chamber liner. Operating conditions of the experiment are shown in Table 1. These could be regarded as some typical conditions of a gross 10kW IGFC system off-gas. Reynolds number of the combustor jet is about  $1.5 \times 10^5$ . It means that the flow status in the flame chamber is fully developed turbulence. This makes it convenient to enlarge the combustor for systems larger than 10kW level since the flow field and flame shape is steady under higher Reynolds numbers (Wang et al. 2016).

**Table 1** Operating conditions of experiments for the exhaust gas combustor

	Flow rate (kg/h)	O <sub>2</sub> Flow rate (kg/h)	Exhaust Gas Mole Fraction			
			CO	H <sub>2</sub>	H <sub>2</sub> O	CO <sub>2</sub>
Case1	3.48	0.47	0.069	0.197	0.061	0.673
Case2	3.48	0.69	0.091	0.261	0.061	0.587
Case3	3.45	0.45	0.101	0.169	0.061	0.669

The test rig is shown in Fig. 2. The modeled exhaust gas composed of H<sub>2</sub>, CO and CO<sub>2</sub> is taken as fuel. Gas is firstly mixed in a mixer with heating function, and then enters a steam evaporator from the bottom. At top of the evaporator, saturated vapor fills the room. Fuel together with vapor goes through the evaporator and gets into the combustor. Mole fraction of steam in the fuel could be adjusted by temperature of the evaporator. Exhaust gas component of two systems under different total fuel utilization is shown. Other slight inert components are replaced by CO<sub>2</sub> in this test. Cooling air through cooling chamber could provide forced convective cooling on the liner. Convective coefficient could be controlled by flow rate of air. Exhaust gas is burned with pure oxygen inside the combustor. An industrial gas analyzer with drying function is used to measure CO<sub>2</sub>, O<sub>2</sub> and CO content in flue gas. Accuracies of the analyzer are within 1% of observed value for main species and  $\pm 1$ ppmv for pollutant. To burn CO out, O<sub>2</sub> is excessively supplied by 5% of equivalence quantity. The temperature of the steam evaporator is

kept at 315K. To avoid possible thermal interference, the species mole fraction was tested without outside cooling air. The cooling chamber could act as a radiation protection. Air in cooling chamber could be considered as static. An approximate thermal isolated environment is approached for the flame chamber.

### **3. Computational Method**

#### **3.1 CFD method**

CFD modeling could provide comprehensive information during designing process. A CFD method is used to simulate flame inside the swirling combustor, which has been proved to have good performance by Wang et al. (2015). The authors compared different models and screened according to experiment data. Moreover, in following studies they had verified the model in Re ranged from  $0.32 \times 10^5$  to  $1.12 \times 10^5$  through experiment method, which covered developing and developed flow conditions (Wang et al. 2016). A modified realizable k- $\epsilon$  turbulent model and the eddy-dissipate concept (EDC) combustion model coupled with detailed chemical mechanism are used. Enhanced wall treatment was applied. The physical property is calculated by the transport and thermal package in the chemical mechanism. Ideal gas law is adopted to compute the density of gas. And the specific heat is calculated by the mixing-law. The thermal conductivity and the kinematic viscosity are computed through the ideal-gas mixing-law. Kinetic theory is used to calculate the mass diffusivity and the heat diffusivity. The radiation is simulated by the discrete ordinate (DO) model. The liner wall is set as radiant and convective boundary (Wang et al. 2016). The combustor was 3D modeled in steady state. Commercial software Ansys Fluent is used to solve modeling equations.

To verify the CFD numerical method, a similar standard flame experiment with high reliability is modeled. The burning experiment fueled with methane was carried out by Sydney University, which also contained a swirling diffusion flame jet. The experiment was specifically described in reference (Kalt et al. 2002). The flame temperature of the flame axis was tested to record the flame structures. Case SM1 of the experiments is calculated by the above CFD method. GRI 3.0 scheme is applied to simulate the methane combusting chemical reactions. Results of the flame temperature on the flame center axis are compared with experiment data in Fig.3. A satisfied agreement is shown on flame structure.

The independence verification of grids is shown in Fig.4. The temperature contours of symmetry plane are displayed. Two different series of mesh are used to calculate the flame. In case (a), 200,000 cells are taken for simulation, while 1,000,000 cells for case (b). No notable difference is shown for two different series of mesh. Thus, grids of 200,000 are taken for following calculations for computing resource saving consideration.

#### **3.2. Chemical reactor network method**

The chemical reactor network (CRN) model is usually used to simulate species and temperature fields in a combustor using a detailed chemical kinetic mechanism. The advantage of it is that it can calculate pollutant such as  $\text{NO}_x$ , CO accurately and provide more information for reaction. Because it can simulate finite-rate chemistry effects with detailed kinetic mechanisms for combustion and pollutant formation. The reactor network must be constructed from a converged CFD simulation. The combustor volume is subdivided into a small number of connected reactors. The mass fluxes through the network are determined from the CFD solution. Here, a CRN model for the combustor is established according to CFD results obtained above. The modeling process was reported, verified (Wang et al. 2016) and used (Shao et al. 2017) in previous reports. The model is shown in Fig.5. Perfect stirred reactor (PSR) models upstream are used to simulate the fuel/oxygen unmixedness in primary zone. Reactors downstream simulate the developing zone. The resident time was determined by the flow velocity. Mass transferring among the reactors was decided by element conservation. A detailed chemical mechanism consisting of a syngas combustion scheme and a  $\text{NO}_x$  chemistry scheme is adopted in this study, which was previously verified (Wang et al. 2016). As shown, model B in Fig.5 (b) has more reactors to simulate each flame zones which mean the model is more detailed compared with model A in Fig.5 (a). The CRN is solved in the commercial software Chemkin. CO emission simulation results of experiment cases are shown in Fig.6 compared with experiment data. Agreements between calculation and data are indicated which could prove reliability of the model. No notable difference was shown between the results of model A and B. In following studies, model A was adopt to save some computing resource and species components of Case3 are taken into consideration as examples unless special declaration is made.

## 4. Results And Discussion

### 4.1. Exhaust gas condensation temperature effects on ignition

In anode exhaust gas, moisture level could be extremely high which makes it difficult to gain a steady flame in the combustor. It is mainly because some radical decomposed from  $\text{H}_2\text{O}$  suppresses burning reactions of syngas. Therefore, in IGFC systems, anode exhaust gas should be condensed before oxy-combustor to remove some water. The heat loss of condensation might be recovered by some heat recovering facility. In that case, steam partial pressure at entrance of combustor is determined by the saturated vapor pressure. The condensation temperature  $T_{\text{con}}$  could be considered as the inlet temperature of combustor. A single PSR model is used to study the relationship between the condensation temperature and flame temperature, which is of great importance to flame stability. Ignite temperature is set to 1100K. Resident time is 1s. Results are shown in Fig. 7.

It is shown in Fig. 7 that the equivalence adiabatic flame temperature  $T_{\text{ad}}$  decreases with condensation temperature increasing. It is because moisture content is low under low condensation temperature. If the condensation temperature is higher than 350K, flame temperature is lower than ignition temperature which means too much excess steam existing and failing to ignite. In practical systems, steam could not

be wiped out completely which make  $T_{ad}$  always lower than it without vapor.  $T_{ad}$  under dry condition is around 1700K in Case3. In view of heat loss during burning process, it might be proper to have a  $T_{ad}$  500K higher than ignition temperature to gain a steady flame. Based on above, 315K might be an ideal condensation temperature for system process design where  $T_{ad}$  is about 1680K. This condition could be reached through water chiller.

## 4.2. CO conversion

The most important indicator is the processing capacity for an exhaust gas treating device aiming at CO<sub>2</sub> capture. It could be represented by the dry CO<sub>2</sub> mole fraction in exhaust gas after burning. CO conversion after combustor could be determined by the flame temperature and oxidant quantity. Beside equivalence ratio, heat loss affects flame temperature directly. As mentioned, forced convection is set outside flame chamber to control the liner temperature which would certainly bring heat releasing problem. CFD method is used to calculate the CO<sub>2</sub> mole fraction after treatment under different equivalence ratio and liner air cooling convective coefficient conditions. The cooling air temperature is set as 298K. Nusselt number Nu is attained from the Dittuse-Boelter correlation for fully developed flow:

$$Nu = 0.023Re^{0.8}Pr^{0.4}$$

$$Re = \frac{\rho q d}{\mu A}$$

Here, Re stands for Reynolds number; Pr for Prandtl number;  $\rho$  for density; q for mass flow rate; d for equivalence diameter;  $\mu$  for viscosity; A for sectional area. Simulation results are shown in Fig. 8. Besides, data of experiment above is shown in Table 2.

It shows in Fig.8 that CO<sub>2</sub> mole fraction after burning under dry condition is higher than 0.958 under every calculating cases. The rest of dry flue gas mainly consists of CO, O<sub>2</sub> and other impurity gas. It indicates that the existing combustor performs well in tail gas treating. Cooling convective coefficient seems to show slight effects on CO conversion, which may due to tiny influence to flame temperature caused by liner heat loss. CO mole fraction varies obviously with excess O<sub>2</sub> quantity relatively. This confirms that CO could be almost fully converted under flame burning condition. Excess O<sub>2</sub> decreases the CO<sub>2</sub> mole fraction in flue gas because it does not participate in reaction. Excess O<sub>2</sub> helps CO being burned out which reduces CO emission in consideration of unexpected unmixedness at jet outlets. At this point of view, 5% excess O<sub>2</sub> could be recommended while it does not obviously affect CO<sub>2</sub> mole fraction after burning. The liner forced cooling strength shows little influence on CO conversion. Table 2 shows that CO<sub>2</sub> concentration of dry flue gas after burning is over 0.958, which could be considered as an ideal rate for capture. They would be dried out before capture process. It is experimentally proved that CO can be converted to CO<sub>2</sub> efficiently by oxy-combustion.

**Table 2** Experiment data of CO<sub>2</sub> mole fraction in dry exhaust gas after burning.

Case	CO <sub>2</sub> mole fraction
Case1	0.962
Case2	0.962
Case3	0.958

### 4.3. Liner temperature

Liner temperature of combustor might be another key indicator for oxy-combustor evaluating. Mostly, the liner temperature is strongly influenced by flame temperature distribution. Equivalence ratio might vary in a narrow range for an oxy-combustor aiming at CO<sub>2</sub> capturing. It makes flame temperature range relatively small especially for diffusion flame. Thus, flame temperature distribution is mainly determined by fuel jet form. As mentioned, forced air cooling should get involved outside the liner. In that case, liner temperature is influenced by heat transfer and jet flow form. Heat transfers in from high temperature burning gas and then out to cooling air outside chamber. For anode exhaust gas characterized by extremely low calorific value, strong swirling might be bring in to the flow field organizing inside to stabilize the flame. Tangential angle of fuel jet would affect mass and heat transfer inside liner. Because fuel flow rate could be over 5 times more than oxygen flow rate. Moreover, tangential angle of jet influences mixedness of fuel and oxygen which may affect local flame temperature. Maximum liner temperature is calculated by CFD model under different outside convective coefficient and fuel jet tangential angle. The O<sub>2</sub> flow rate at boundary is set as 5% excessively compared with equivalent quantity. Results are shown in Fig.9.

Max liner temperature decreases with the outside convective coefficient, which proves that forced convection outside flame chamber is an effective way to protect the combustor. It can be noticed that max liner temperature has an optimal value at tangential angle around 25°. Main reason for this might be as following. Stronger swirling makes a better mixing condition. When jet tangential angle is around 20°, mixing between fuel and oxygen is not desirable. High level of unmixedness leads flame to burning under low equivalence ratio, which causes high local temperature. Liner temperature increases when local temperature is high. When jet tangential angle is around 30°, larger centrifugal force makes high temperature gas scour liner more fiercely which may cause high liner temperature, although mixing level is more desirable. It can be inferred that an optimal tangential angle, which could vary with dimensions of combustor, exists for liner temperature controlling.

### 4.4. Pollutant emissions

Pollutant emission is always an important indicator for different kinds of power plants. Differing from traditional plants, electrochemical reactions inside SOFC may cut pollutant formation during fuel utilizing process. However, oxy-combustor adds burning step into systems which may cause some emission problem. Generally speaking, O<sub>2</sub> production from cryogenic air separation unit (ASU) may usually contain

$N_2$  up to 5% by volume. Therefore, in practical IGFC system, some  $N_2$  always exists in syngas even though  $O_2$  gasification technology might be involved. So combustor pollutant is mainly consisting of CO and  $NO_x$ . The above CRN model, which is established according to CFD results of 25° jet swirl angle, is used to compute pollutant emissions of the oxy-combustor. Case2 and Case3 are computed and compared. It could be indicated that the fuel utilization ratio of Case2 is lower than that of Case3 because Case2 contains more combustible components. As shown above, this leads to a difference between components of exhaust gas. In this period, exhaust gas contains 3%  $N_2$  by volume in simulation case. Ratio of other component is kept as before. Emissions under different excess  $O_2$  quantity are computed under thermal isolated condition, which is similar to the experiment. Comparison of combustion with pure  $O_2$  and industrial  $O_2$  containing 5%  $N_2$  was also applied to figure out the oxygen purity impacts on emissions. Results are shown in Fig. 10 and Fig. 11. It could be considered that  $H_2$  has been completely converted to water after direct flame burning because  $H_2$  has extremely high burning rate compared with CO especially under pure oxygen condition. To make the calculations comparable, all the results have been corrected to numbers at 3%  $O_2$  concentration under dry condition.

It is shown that both CO and  $NO_x$  emissions decrease with rising of excess  $O_2$  percent. It is known that  $NO_x$  formation is directly related to flame temperature. When excess  $O_2$  percent is low, local flame temperature could be higher which leads to higher  $NO_x$  emissions. On the other side, more excess  $O_2$  supply makes CO burnt more completely which means lower CO emissions. Therefore, excess  $O_2$  supply is in favor of pollutant reducing. Combined with mentioned, if  $CO_2$  concentration could meet the requirement of  $CO_2$  capturing,  $O_2$  should be supplied as more as possible. The exit temperature of combustor could be regard as the same because the difference of excess  $O_2$  is not very notable. Case2 releases more CO and  $NO_x$  than Case3. It is because that Case2 has a lower total utilization rate of 80% in fuel cells which means exhaust gas contains more combustible component. Flame temperature of Case2 is about 2000K whereas it is 1650K for Case3. High temperature leads to high  $NO_x$  emission. Besides, Case2 contains more  $H_2$  so that  $H_2O$  mole fraction is high after burning. Vapor and  $H_2$  enrichment in fuel prevents CO converting to  $CO_2$  especially under high temperature, which leads to high CO emission level (Wang et al. 2016). Main reasons for this are as follow. Vapor has a larger heat capacity and declines flame temperature. H radical suppressed CO converting through the reaction . The experiment data above also shows some agreement to that. As known,  $NO_x$  formation increases extremely when temperature exceeds 1800K. It could be concluded that for system design, total fuel utilization percent had better be high enough to make oxygen flame temperature of anode exhaust gas lower than 1800K, which make systems environment friendly.  $NO_x$  emissions increase when oxygen purity decreases. And CO emissions showed slightly decline with oxygen purity decreasing. But the impacts of oxygen purity on  $NO_x$  and CO are not notable. This is mainly because flow rate of oxygen is relatively small compared with that of exhaust gas. Thus,  $N_2$  importing with oxygen flow is rather small and could not influence total  $N_2$  concentration obviously. As  $N_2$  does not participate in CO oxidizing reactions, rarely difference is shown under different  $O_2$  purity conditions.

Liner cooling can affect pollutant emissions. Emissions under different cooling conditions are calculated. Results are shown in Fig.12. Liner cooling protects flame chamber from damage of high temperature. However, it would certainly decrease the flame temperature inside flame chamber. The combustor exit temperature with a convective coefficient of  $17.5 \text{ W/m}^2$  decrease compared with that of heat isolation case. The reacting temperature declining leads to a lower CO and higher  $\text{NO}_x$  emissions.

## 5. Conclusions

In this work, an oxy-combustor is studied through experiment, CFD and CRN simulation method under different system processing conditions. The simulation method could be verified by experiment data. Then some key indicators of the combustor including exhaust gas condensation temperature impacts on ignition, CO conversion, and liner temperature and pollutant emissions are discussed. Main conclusions are as follow:

Anode exhaust gas should be condensed before oxy-combustor to remove some water. For Case3 which contains least  $\text{H}_2$ ,  $T_{ad}$  under dry condition is around 1700K. Considering heat loss in practical system, 315K might be an ideal condensation temperature for system process design where  $T_{ad}$  is about 1680K. It would be a key index for the IGFC with  $\text{CO}_2$  capturing integrated system process designing.

$\text{CO}_2$  mole fraction after burning under dry condition is higher than 0.958 with excess  $\text{O}_2$  less than 5%. Convective coefficient seems to show slight effects on CO conversion. It is confirmed that CO could be almost fully converted under flame burning condition and unreactive  $\text{O}_2$  existing decreases the  $\text{CO}_2$  mole fraction. 5% excess  $\text{O}_2$  could be recommended to help CO burning out while it does not obviously affect  $\text{CO}_2$  mole fraction after burning. The liner forced cooling strength shows little influence on CO conversion. It is proved that direct flame burning is an effective and reliable way to accomplish  $\text{CO}_2$  concentrating for IGFC system. Oxy-combustor could be used in industrial systems.

For an oxy-combustor aiming at  $\text{CO}_2$  capturing, total flame temperature range relatively small because off-gas is almost burnt under equivalence ratio to achieve  $\text{CO}_2$  gathering. Liner temperature is influenced by heat transfer outside and jet form. Force convection outside flame chamber is an effective way to protect the combustor. When jet tangential angle is smaller, high level of unmixedness between fuel and oxygen leads to high temperature. While jet tangential angle is larger, centrifugal force makes high temperature gas scour liner more fiercely. Max liner temperature has an optimal value at jet tangential angle around  $25^\circ$ . These conclusions might be of guiding significance for combustor design.

Both CO and  $\text{NO}_x$  emissions decrease with rising of excess  $\text{O}_2$  percent. When excess  $\text{O}_2$  percent is low, more  $\text{NO}_x$  releases due to high flame temperature. While excess  $\text{O}_2$  supply makes CO burning more completely. If  $\text{CO}_2$  concentration could meet the requirement of  $\text{CO}_2$  capturing,  $\text{O}_2$  should be supplied as more as possible. Purity of  $\text{O}_2$  barely influenced the pollutant emissions. The liner cooling intensity

decrease flame temperature. The temperature declining leads to a lower CO and higher NO<sub>x</sub> emissions. For system design, total fuel utilization percent had better be high enough to make oxygen flame temperature of anode exhaust gas lower than 1800K, which make systems environment friendly.

## References

- Thallam Thattai A, Oldenbroek V, Schoenmakers L, Woudstra T, Aravind P, 2017. Towards retrofitting integrated gasification combined cycle (IGCC) power plants with solid oxide fuel cells (SOFC) and CO<sub>2</sub> capture – A thermodynamic case study. *Applied Thermal Engineering* 114, 170-185.
- Wu Z, Zhu P, Yao J, Tan P, Xu H, Chen B, Yang F, Zhang Z, Ni M, 2020. Thermo-economic modeling and analysis of an NG-fueled SOFC-WGS-TSA-PEMFC hybrid energy conversion system for stationary electricity power generation. *Energy* 192, 116613.
- Al-Khori K, Bicer Y, Koc M, 2020. Integration of solid oxide fuel cells into oil and gas operations: needs, opportunities, and challenges. *Journal of Cleaner Production* 245, 118924.
- Pirasaci T, 2019. Non-uniform, multi-stack solid oxide fuel cell (SOFC) system design for small system size and high efficiency. *Journal of Power Sources* 426, 135-142.
- Ferreira T, Wuillemin Z, Faulwasser T, Salzmann C, Van herle J, Bonvin D, 2019. Enforcing optimal operation in solid-oxide fuel-cell systems. *Energy* 181, 281-293.
- Wang X, Lv X, Weng Y, 2020. Performance analysis of a biogas-fueled SOFC/GT hybrid system integrated with anode-combustor exhaust gas recirculation loops. *Energy* 197, 117213.
- Spallina V, Nocerino P, Romano M C, Annaland M S, Campanari S, Galluci F, 2018. Integration of solid oxide fuel cell (SOFC) and chemical looping combustion (CLC) for ultra-high efficiency power generation and CO<sub>2</sub> production. *International Journal of Greenhouse Gas Control* 71, 9-19.
- Francisco J, Alvarez G, Gonzalo de Grado J, 2016. Study of a modern industrial low pressure turbine for electricity production employed in oxy-combustion cycles with CO<sub>2</sub> capture purposes. *Energy* 107, 734-747.
- Chen X, Xu Z, Yang F, Zhao H, 2019. Flame spray pyrolysis synthesized CuO-TiO<sub>2</sub> nanoparticles for catalytic combustion of lean CO. *Proceeding of the Combustion Institute* 37, 5499-5506.
- Han S W, Kim H D, Jeong M, Park K J, Kim Y D, 2016. CO oxidation catalyzed by NiO supported on mesoporous Al<sub>2</sub>O<sub>3</sub> at room temperature. *Chemical engineering journal* 283, 992-998.
- Dey S, Dhal G C, 2020. Property and structure of various platinum catalysts for low-temperature carbon monoxide oxidations. *Material today chemistry* 16, 100288.

- Ilbas M, Bektas A, Karyeyen S, 2019. A new burner for oxy-fuel combustion of hydrogen containing low-calorific value syngases: an experimental and numerical study. *Fuel* 256, 115990.
- Rashwan S S, Ibrahim A H, Abou-Arab T W, Nemitallah M A, Habib M A, 2017. Experimental study of atmospheric partially premixed oxy-combustion flames anchored over a perforated plate burner.
- Imteyaz B A, Nemitallah M A, Abdelhafez A A, Habib M A, 2018. Combustion behavior and stability map of hydrogen-enriched oxy-methane premixed flames in a model gas turbine combustor. *International journal of hydrogen energy* 43, 16652-16666.
- Li B, Shi B, Zhao X, Ma K, Xie D, Zhao D, Li J, 2018. Oxy-fuel combustion of methane in a swirl tubular flame burner under various oxygen contents: operation limits and combustion instability. *Experimental thermal and fluid science* 90, 115-124.
- Ning D, Wang S, Fan A, Yao H, 2018. A numerical study of the effects of CO<sub>2</sub> and H<sub>2</sub>O on the ignition characteristics of syngas in a micro flow reactor. *International journal of hydrogen energy* 43, 22649-22657.
- Topal A, Turan O, 2019. One dimensional liner temperature prediction in a tubular combustor. *Energy* 171, 1100-1106.
- Schluckner C, Gaber C, Landfahner M, Demuth M, Hochenauer C, 2020. Fast and accurate CFD-model for NO<sub>x</sub> emission prediction during oxy-fuel combustion of natural gas using detailed chemical kinetics. *Fuel* 264, 116841.
- Khallaghi N, Hanak D P, Manovic V, 2020. Techno-economic evaluation of near-zero CO<sub>2</sub> emissions gas-fired power generation technologies: A review. *Journal of natural gas science and engineering*, 74, 103095.
- Wang H, Shao W, Lei F, Zhang Z, Liu Y, Xiao Y, 2016. Experimental and numerical studies of pressure effects on syngas combustor liner temperature. *Applied thermal engineering* 82, 30-38.
- Wang H, Lei F, Shao W, Xiong Y, Zhang Z, Xiao Y, 2015. Screening and modification of CFD models for syngas turbine combustor. *Proceedings of CSEE* 6, 1429–1435. (in Chinese)
- Wang H, Lei F, Shao W, Zhang Z, Liu Y, Xiao Y, 2016. Experimental and numerical studies of pressure effects on syngas combustor emissions. *Applied thermal engineering* 102, 318-328.
- Kalt P, Al-Abdeli Y, Masri A, Barlow R, 2002. Swirling turbulent non-premixed flames of methane: flow field and compositional structure. *Proceedings of the Combustion Institute* 29(1), 1913–1919.
- Shao W, Zhao Y, Liu Y, Wang H, Tian Y, Lu Y, Zhang Z, Xiao Y, 2017. Investigation of fuel/air mixing uniformity in a natural gas premixed burner for gas turbine combustor applications. *Proceedings of CSEE* 3, 795-802. (in Chinese)

# Figures

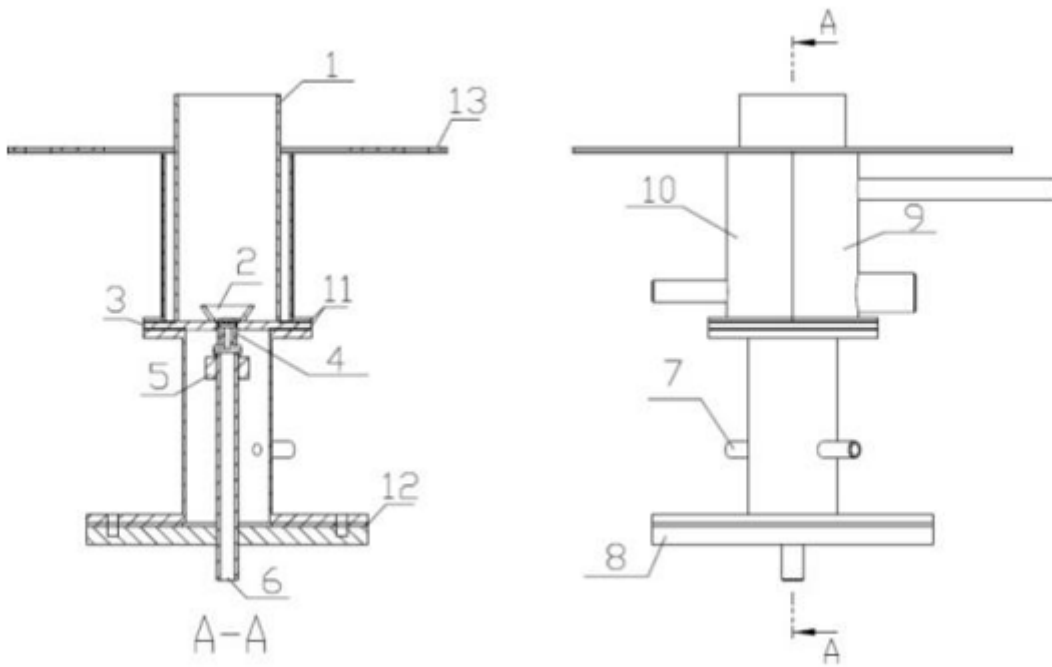


**Figure 1**

Exhaust gas concept oxy-combustor for 10kW IGFC system (1. flame chamber 2. flame stabilizer 3. oxygen swirler 4. fuel swirler 5. connector 6. fuel pipe 7. oxygen pipe 8. base plate 9-10. cooling air chamber 11-13. sealing material)

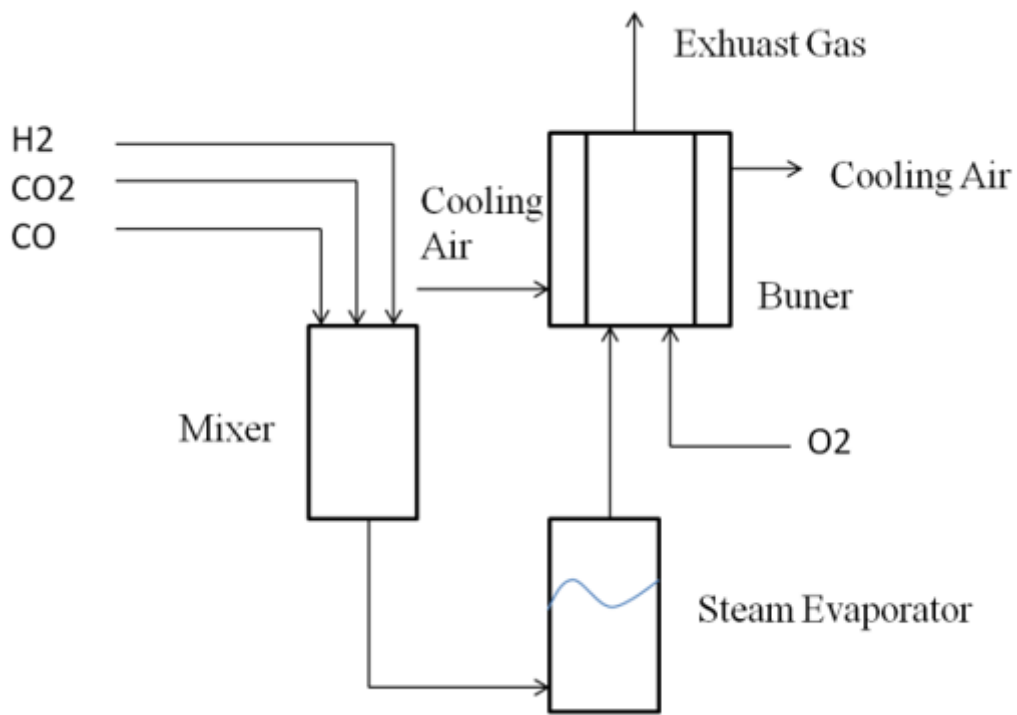


Figure 2

Exhaust gas combustion test rig

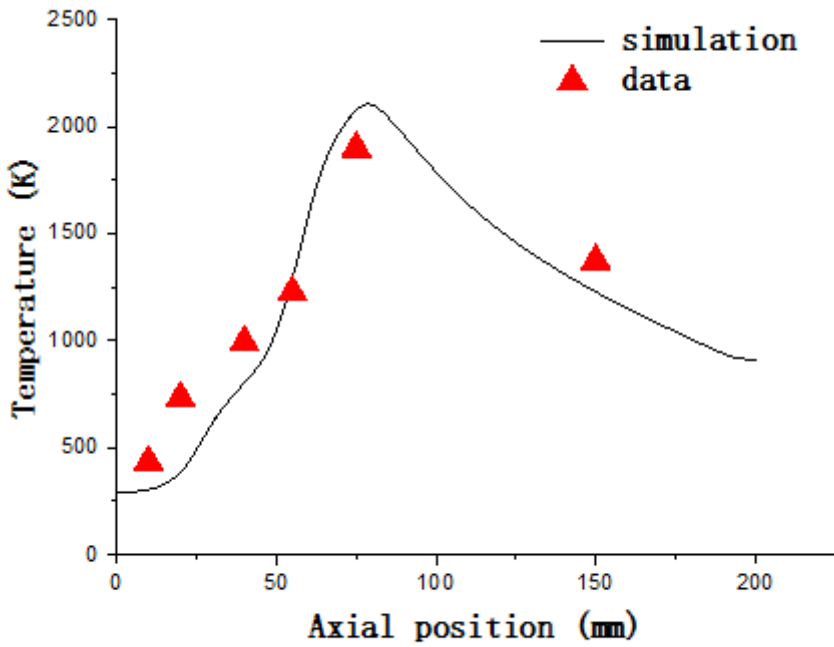
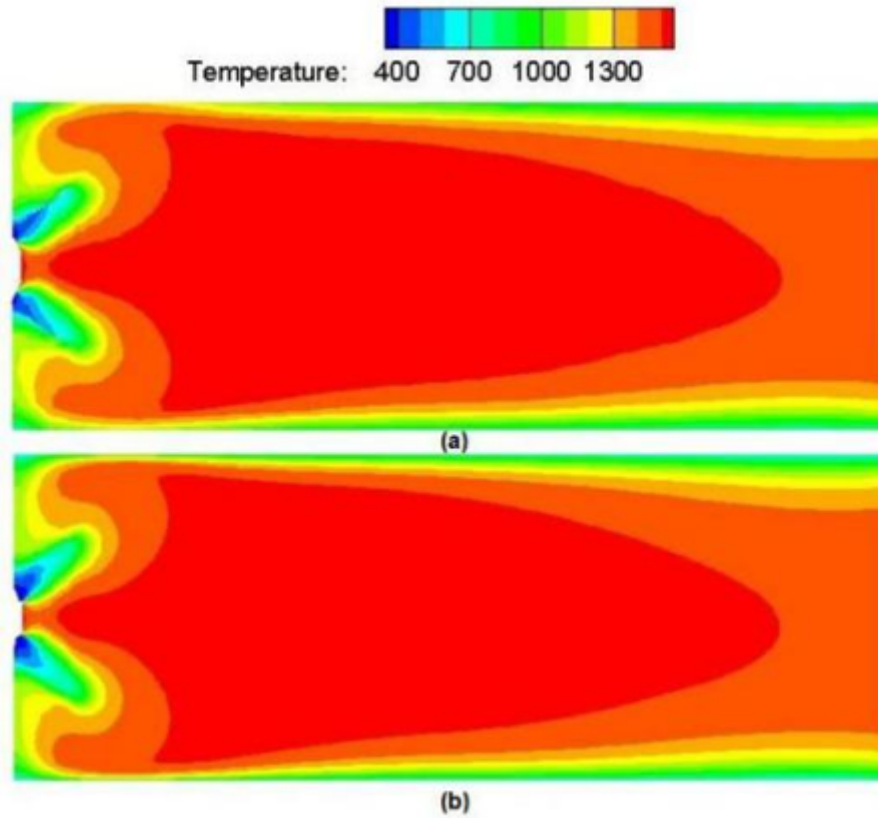
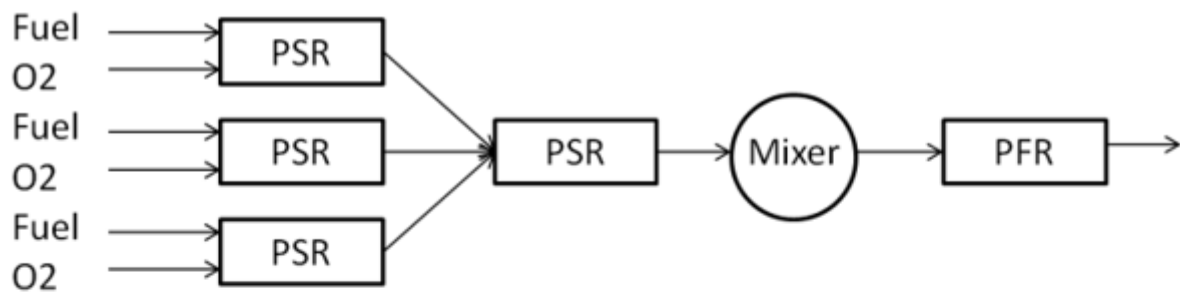


Figure 3

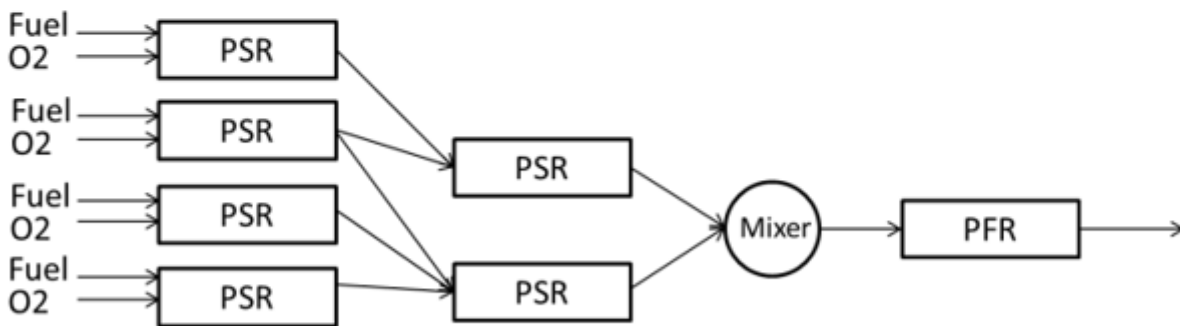


**Figure 4**

Temperature distribution through CFD under different mesh density ((a) for 200,000 cells; (b) for 1,000,000 cells)



**(a) model A**



**(b) model B**

**Figure 5**

Chemical reactor network model for the combustor.

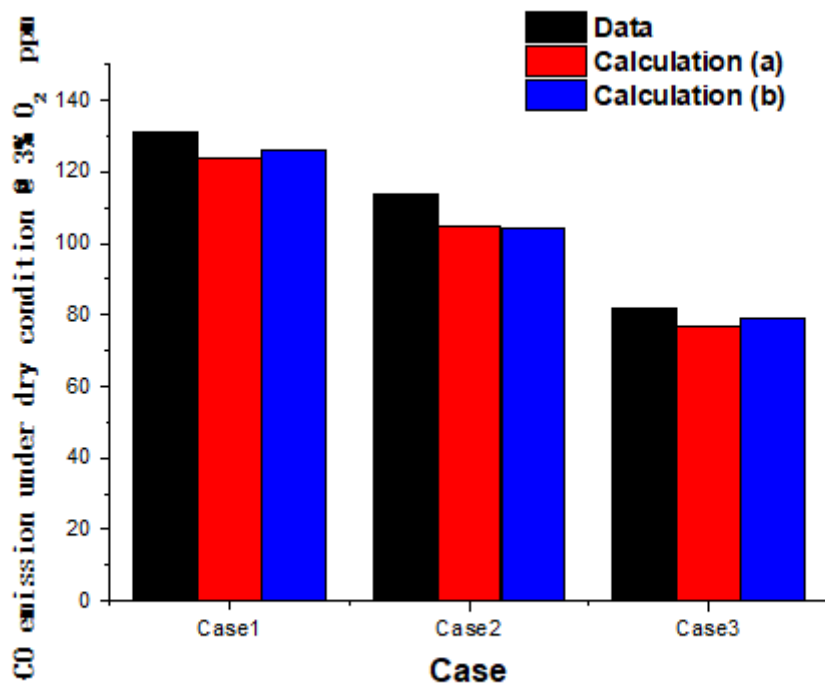


Figure 6

Comparison between calculation and experiments.

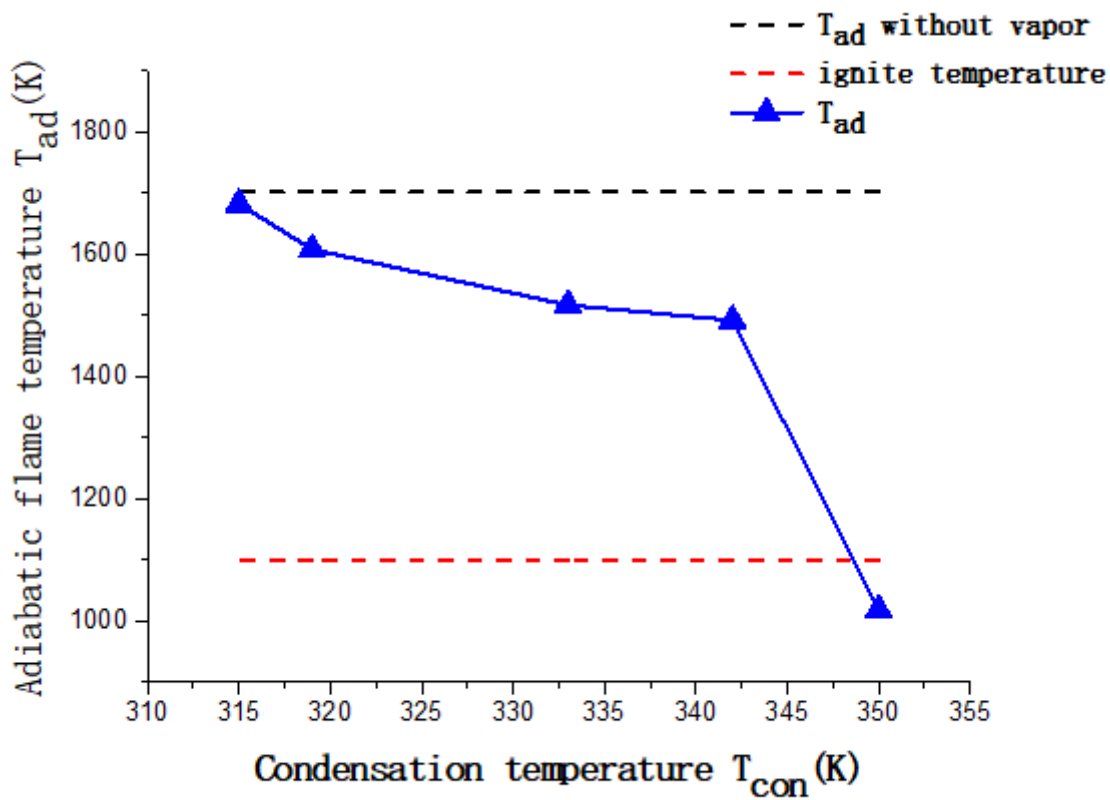


Figure 7

Equivalence adiabatic flame temperature of exhaust gas under different condensation temperature.

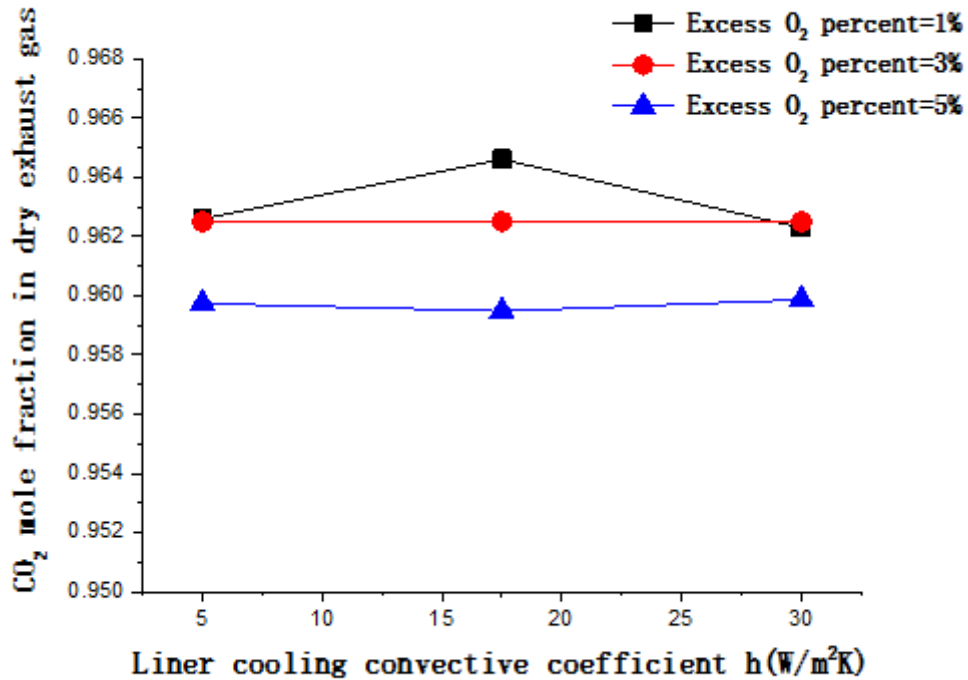


Figure 8

CO2 mole fraction in dry exhaust gas after burning by CFD calculation.

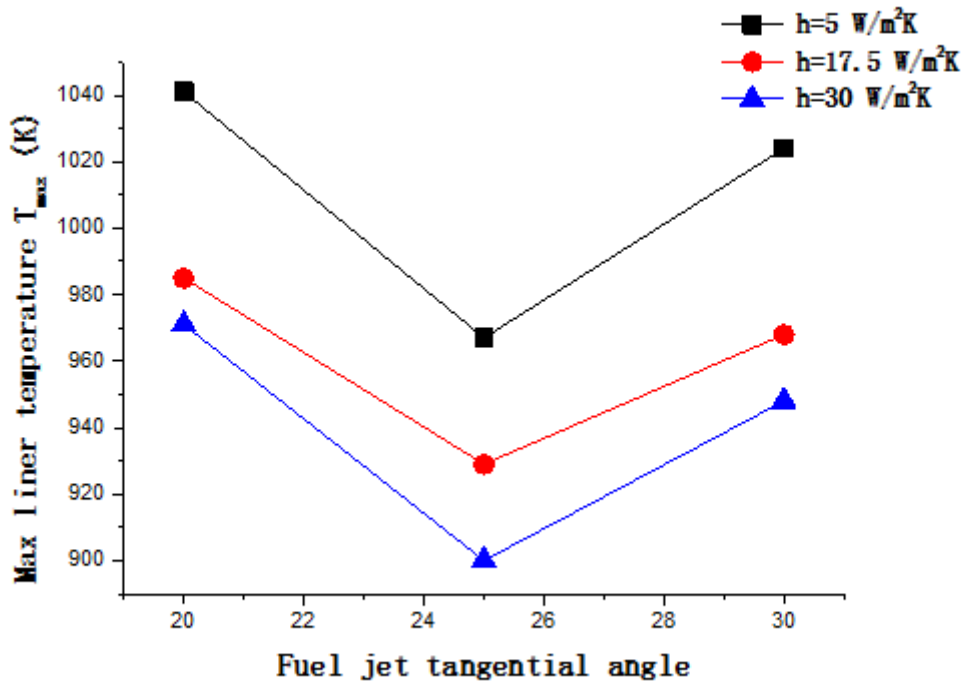
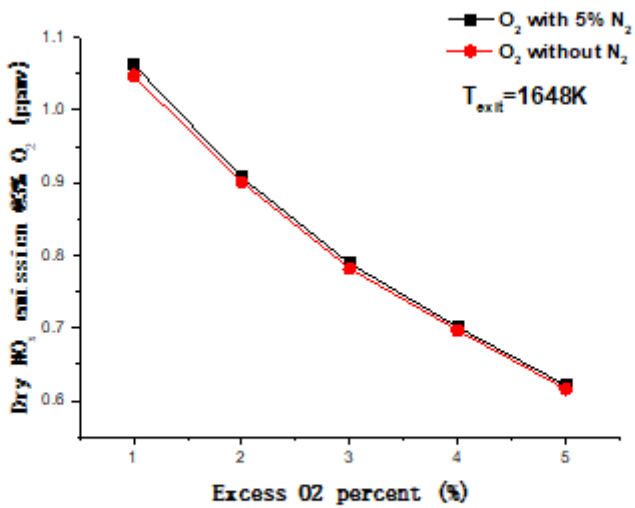
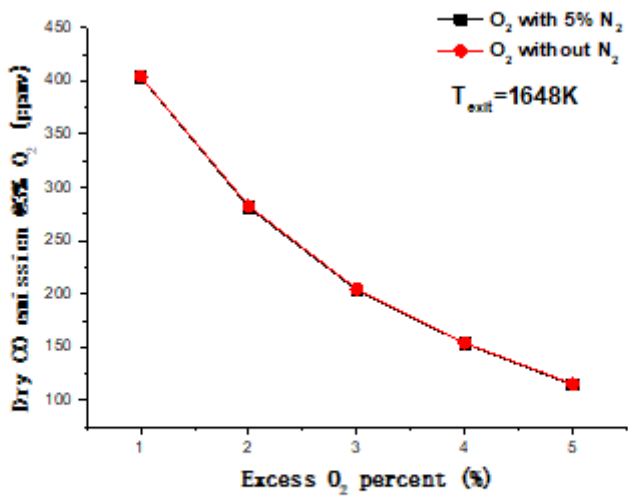


Figure 9

Maximum temperature of combustor liner under different condition by CFD calculation.



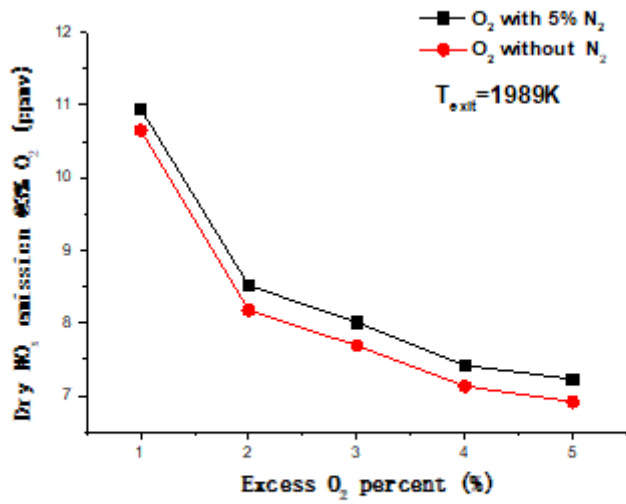
(a)  $\text{NO}_x$  emissions



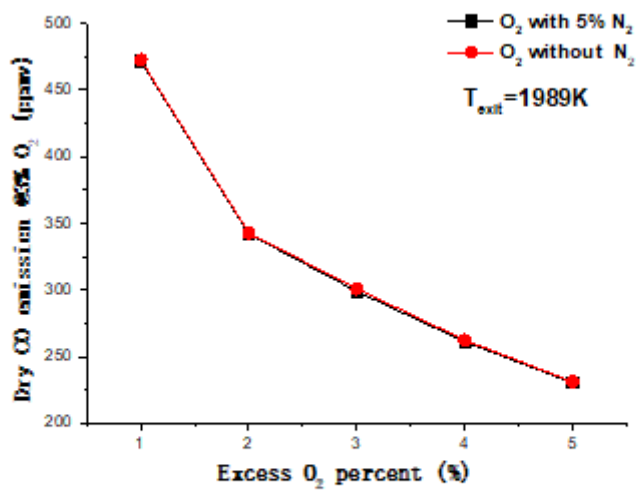
(b) CO emissions

Figure 10

Computed pollutant emissions of Case3 by CRN model.



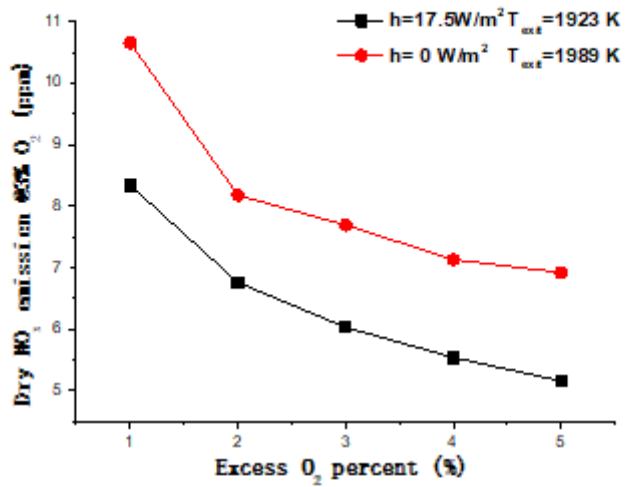
(a) NO<sub>x</sub> emissions



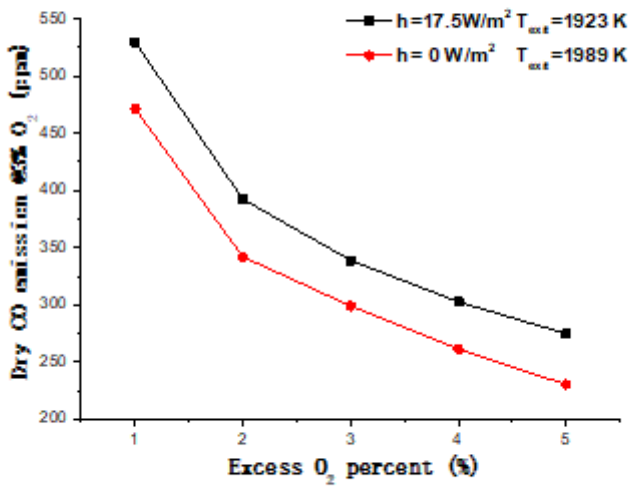
(b) CO emissions

Figure 11

Computed pollutant emissions of Case2 by CRN model.



(a) NO<sub>x</sub> emissions



(b) CO emissions

Figure 12

Computed pollutant emissions of Case2 by CRN model.